Vibrational state control of bimolecular reactions

Christoph Kreher
Institut für Physikalische Chemie, Universität Zürich, Winterthurerstr, 190, CH-8057 Zürich, Switzerland

Jan Leo Rinnenthal and Karl-Heinz Gericke
Institut für Physikalische und Theoretische Chemie, Technische Universität Braunshweig, Hans-Sommer-Strasse 10, D-38106 Braunschweig, Germany

(Received 31 July 1997; accepted 10 November 1997)

The influence of rotation and vibration on the reactivity and the dynamics of the reaction $X+HCN(\nu_1,\nu_2,\nu_3,J)\rightarrow HX+CN(v,J)$ with X=H, Cl has been studied. The HCN molecule is prepared in a specific rovibrational level by IR/VIS overtone excitation in the wavelength region 6500–18 000 cm^{-1}. The H atoms are generated by laser photolysis of CH_3SH at 266 nm, the Cl atoms are formed in the photodissociation of Cl_2 at 355 nm. The CN products are probed quantum state specifically by laser-induced fluorescence (LIF). For low rotational states of HCN, the reactivity of Cl and H is independent of the initial rotational state. However, an enhancement in reactivity of the Cl+HCN reaction is observed when the time of rotation becomes comparable to the passing time of the Cl atom. The reaction of Cl as well as of the H atom with HCN shows strong mode specific behavior, implying a simple direct reaction mechanism, which is also supported from Rice–Ramsperger–Kassel–Marcus (RRKM) calculations. An increase in CH stretch vibration increases both the reaction rate and the CN product vibration. Channeling energy in CN stretch vibration has only a minor effect on the reactivity and the CN product vibration even decreases. Trajectory calculations of the H+HCN system agree with the experimental results. The dependence of reaction rates on reactant approach geometry is investigated by preparing aligned reactants using linear polarized light. The CN signal is markedly influenced by the prepared alignments (steric effect). The experimental results suggest that the reaction of hydrogen and chlorine atoms with vibrationally excited HCN proceeds mainly via a collinear transition state, but the cone of acceptance is larger for chlorine atoms. © *1998 American Institute of Physics.*
[S0021-9606(98)00507-8]

I. INTRODUCTION

Controlling the course of a chemical reaction is an important goal in molecular dynamics.[1] A simple approach is the control of motion of one reactant, which is directed along the reaction coordinate of the bimolecular reaction. This motion along the reaction coordinate corresponds to the motion of the nuclei which carries the system from the reactants to the products. There are several experiments of how reactant vibration affects reactivity and product energy release of the desired bimolecular reaction.[1] In particular, the preparation of HOD in two different distinct vibrational states of pure OH or OD stretches leads to different photodissociation[1–4] and reaction channels.[1,5–7] Crim and co-workers[8] investigated the photodissociation of HNCO, where vibrational excitation of the second overtone of the NH stretch leads to a break of the NH bond at energies below the threshold for the high energy NH+CO channel. At higher energies both channels compete. Rosenwaks and co-workers[9] have demonstrated a rotational state selectivity in bond fission of C_2HD, where the production of H and D atoms depends on the rotational state of the $5\nu_1$ mode.

The present investigation extends the approach of controlling chemical reactions to the endothermic reactions of hydrogen and chlorine with HCN:

$$Cl+HCN(\nu_1,\nu_2,\nu_3,J)\rightarrow HCl+CN, \quad (1)$$

$$H+HCN(\nu_1,\nu_2,\nu_3,J)\rightarrow H_2+CN. \quad (2)$$

The Cl+HCN→HCl+CN reaction is 94 kJ/mol endothermic,[10] has a total barrier of 113 kJ/mol,[11] and has been studied experimentally[11,12] as well as theoretically.[13,14] *Ab initio* calculations by Harding[13] show that the Cl+HCN→HCl+CN reaction proceeds through a linear transition state. They predict a simple, direct collinear abstraction mechanism without complex formation (ClHCN). Sims and Smith[12] have reported experimental studies of the reverse reaction (1), CN+HCl→products, by exciting either CN or HCl vibration. While there is a negligible enhancement of the reaction rate when exciting CN by one quantum of vibration, the rate increases by more than two orders of magnitude when HCl is excited into the first vibrational state. They concluded that CN behaves like a spectator without participation in the reaction.

The reaction of H+HCN→H_2+CN is endothermic by 90 kJ/mol[10] with a total barrier of 112 ± 3 kJ/mol.[15] *Ab initio* calculations by Bair and Dunning[16] predict that the H-atom reaction also proceeds via a linear transition state, which is consistent with the experimental results of Lambert *et al.*[17] and Johnston *et al.*[18] who observed rotationally unexcited CN from the reaction of HCN with translationally hot H atoms. Experimental studies of the reverse H_2+CN reaction report that the reaction rate is unaffected by vibrationally

TABLE I. Band origins ν_0 (cm^{-1}), wavelengths (nm), absolute intensities A ($cm\,mol^{-1}$), and excitation conditions for different overtone bands of HCN.

Overtone	ν_0/cm^{-1}	λ/nm	$A/cm\,mol^{-1}$	Pulse energy dye
(002)←(000)	6519.61[a]	1533.4	$8.499(54)\times10^{4}$[a]	15 mJ DCM[f]
(004)←(000)	12 635.89[a]	791.18	157(1)[a], 154(2)[b]	40 mJ LDS 765
(302)←(000)	12 657.88[a]	789.81	9.11(25)[a], 9.7(2)[b]	40 mJ LDS 765
(402)←(000)	14 653.66[a]	682.24	8.33(10)[a]	90 mJ Pyridin 1
(104)←(000)	14 670.45[a]	681.46	9.42(9)[a]	90 mJ Pyridin 1
(005)←(000)	15 551.94[a]	642.83	17.5(4)[a]	100 mJ DCM
(502)←(000)	16 640.31[c]	600.79	0.40(4)[c]	50 mJ DCM/Rhodamin 6G
(204)←(000)	16 674.21[e]	599.57	1.7(1)[c]	50 mJ DCM/Rhodamin 6 G
(105)←(000)	17 550.42[d]	569.63	3.51(17)[c], 13.9(4)[a]	120 mJ R6G
(006)←(000)	18 377.01[d]	544.01	2.61(13)[c], 2.4(2)[a]	90 mJ Fluorescein

[a]Reference 30.
[b]Reference 32.
[c]Reference 34.
[d]Reference 35.
[e]Reference 36.
[f]Frequency mixing with 1.064 μm.

excited CN.[19] On the other hand, vibrational excitation of H_2 should increase the reaction rate according to theoretical studies.[20] Both the experimental and theoretical results suggest, comparable to the Cl atom reaction, that in the H+HCN reaction the CN bond is unaffected during the reactive encounter.

There have been several experiments on the reactions with high vibrationally excited HCN.[21–24] Crim *et al.*[23,24] examined the reaction dynamics of two vibrational states of HCN, the (004) state in which four quanta of CH stretch are excited and the (302) state in which three quanta of CN stretch and two quanta of CH stretch are excited. Their conclusions are that the H atom reaction forms CN primarily by a direct abstraction reaction and the Cl atom reaction forms CN by an addition–elimination mechanism in addition to the direct abstraction. We have previously reported the reactivity of several different vibrational states of HCN with Cl and H.[21] HCN was excited to the overtone levels (002), (004), (302), (105), and (11^15) with energies up to 18 000 cm^{-1}. We excluded the pure spectator model for both the reaction of Cl+HCN and of H+HCN, because some memory of the reactant initial state is retained in the product.

The present paper now represents a continuation of that study in terms of its mode specific behavior with new insights in the reaction dynamics. While in all former studies a long living intermediate complex could not be excluded the present experiment in conjunction with trajectory studies indicates a rather direct reaction where only a few vibrational motions within the intermediate take place before it breaks apart.

We have been able to excite several more HCN overtone bands and report the state-to-state dynamics of the prepared HCN(ν_1,ν_2,ν_3,J) with hydrogen and chlorine atoms. In particular, we prepared the HCN molecule in the (002), (004), (302), (402), (104), (005), (502), (204), (105), and (006) states. In addition, we analyzed the effect of reactant rotational excitation on the reaction rate as well as on the rotational distribution of the CN product. We also investigated the dependence of reaction rates on reactant approach geometry. This was performed by preparing aligned reactants using linearly polarized laser light. Such experiments give detailed insight into the stereochemistry of the desired bimolecular reaction.

II. EXPERIMENT

The experimental apparatus has been described in detail previously.[21] Briefly, the HCN is synthesized by heating a mixture of KCN and stearic acid under vacuum to ~100 °C. Translationally excited chlorine atoms were generated from Cl_2 in a pulsed laser photolysis with 20–40 mJ of 355 nm light (Quanta Ray DCR1A). The photolysis leads to 98% of the chlorine atoms in the $^2P_{3/2}$ ground spin–orbit state with an anisotropy of $\beta=-1\pm0.1$.[25] Only minor amounts of Cl atoms are generated in the upper $^2P_{1/2}$ state and, thus, no reliable estimation of the role of different Cl spin–orbit states can be obtained. The mean collision energy of the Cl+HCN system is $E_{coll}=25$ kJ/mol. The precursor of H atoms is methanethiol, dissociated at 266 nm light generated from the fourth harmonic of a Nd:YAG laser (15 mJ). The photodissociation yields exclusively H atoms with a mean translational energy of 80 kJ/mol. The anisotropy at 266 nm is not known, but results at 248 nm ($\beta=-1$)[26] and 274 nm ($\beta=-0.86\pm0.05$)[27] suggest that the value is close to -1. The reactants (CH_3SH/Cl_2 and HCN) were mixed in the reaction chamber by separate nozzles. The partial pressures were $P(Cl_2)=8$ Pa and $P(CH_3SH)=P(HCN)=16$ Pa.

A Nd:YAG laser pumped dye laser (Continuum YG 680, TDL 60, IRP) with a pulse width of typically 7 ns at a bandwidth (FWHM) of 0.07–0.09 cm^{-1} excites the vibrational states of HCN. All wavelengths in the near infrared and visible (IR/VIS) region were obtained using different laser dyes (Table I). Probing the (002)←(000) overtone band of HCN in the infrared region near 1.53 μm was performed via difference frequency mixing of a dye laser and a 1.064 μm Nd:YAG laser beam.

Nascent CN products were detected applying the laser-induced fluorescence (LIF) technique via the

$B\ ^2\Sigma^+ \leftarrow X\ ^2\Sigma^+$ $(\Delta v = 0)$ band. The required radiation around 388 nm was supplied by a dye laser (Lambda Physik FL2002, QUI) pumped by a XeCl excimer laser (Lambda Physik EMG 101 MSC). All LIF spectra were detected with 2–5 mJ of laser light under saturated conditions. A photomultiplier (THORN-EMI 9781B) monitored the LIF signal perpendicular to the probe beam through $f/1$ optics and an interference filter (389 ± 10 nm). All lasers were operated at a repetition rate of 10 Hz. The time delay between the photolysis laser, which is in time with the IR/VIS excitation laser, and the LIF-probe laser was set between 50 and 150 ns.

The overlap of the laser beams was optimized by the CN signal. The spectral range of the dyes was sufficient to excite different (ν_1, ν_2, ν_3) vibrational modes. Thus the CN product intensities originating from different HCN(ν_1, ν_2, ν_3) reactants can be easily compared. No ''beam walk'' effects were observed.

III. RESULTS AND DISCUSSION

A. Vibrational state control of the reaction rate

In order to study the influence of the initial vibrational state of HCN on the reaction rate with chlorine atoms, the yield of CN $(\nu = 0,\ J = 8)$ products was monitored while the HCN excitation laser light was tuned to separated rotational transitions in the different vibrational bands. The CN was detected at a fixed wavelength via the $R(8)$ line. Using the absorption cross section[28–36] for vibrational overtone excitation A and the power density of the HCN excitation laser I, we convert the CN signals S to relative rates k. In case of a small time delay the ratio of rate constants k_1/k_2 between two vibrational states of HCN is given by

$$\frac{k_1}{k_2} = \frac{S_1}{S_2} \cdot \frac{I_2}{I_1} \cdot \frac{P_2}{P_1} \cdot \frac{A_2}{A_1}, \tag{3}$$

where $P_i = P_i(\nu, J)$ is the CN product state population in the (ν, J)-rovibrational state. In case that the excitation energies between the desired vibrational states are close together, it is relatively easy to obtain the ratio of rate constants by measuring an action spectrum of HCN. Figure 1 shows the CN signal (lower part) from the reaction HCN+Cl→HCl+CN as a function of the excitation wavelength and a simulation (upper part) using the known HCN Franck–Condon and Hönl–London factors.[32] The main peaks in the wavelength region near 792 nm are due to rotational transitions from the vibrational ground state to the (004) vibrational state. Several less intense rotational lines are transitions to a (302) vibrational state of HCN, containing two quanta of CH stretch and three quanta of CN stretch. By comparing the intensities in the action spectra with the corresponding intensities from the simulation, we find a ratio of rate constants between HCN(004) and HCN(302) of $k(004)/k(302) = 2.8 \pm 0.6$.[21] The reaction rate of Cl with HCN is enhanced when the energy is located in the reaction coordinate (the CH stretch) instead of locating the same amount of energy in three quanta of CN and two quanta of CH stretch. A similar mode

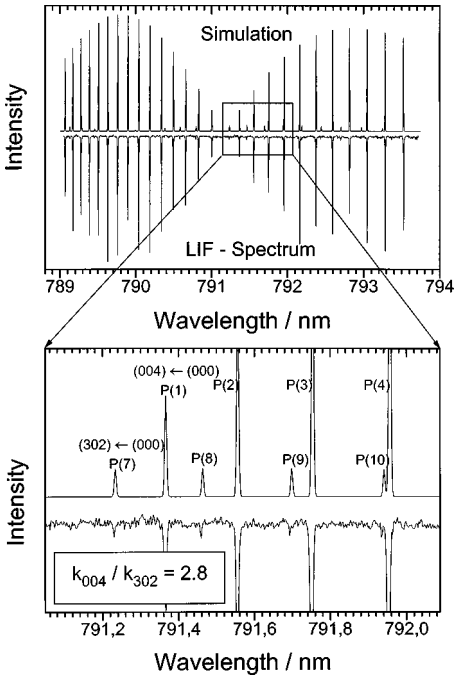

FIG. 1. Comparison of an action and a simulation spectrum for the Cl+HCN reaction. The HCN excitation laser is tuned over the (004) ←(000) and (302)←(000) bands. The observed intensities of transitions originating from the (302) vibrational state are lower than those of the simulation.

selectivity was found in the reaction of HCN+H→H_2+CN. We previously reported a lower limit of the ratio of rate constants of $k(004)/k(302) > 4$.[21]

This result agrees with theoretical results obtained by Bair and Dunning.[16] They found that the endothermic reaction has a collinear saddle point with a CH distance of 1.55 Å, compared to the equilibrium bond distance of 1.06 Å in the HCN molecule (late barrier). The CN distance is essentially constant being 1.16 Å in HCN, 1.18 Å (calc) at the saddle point, and 1.17 Å in free CN. This implies that the reaction will only be substantially accelerated if the CH stretch is vibrationally excited. Similar theoretical results were found for the Cl+HCN reaction by Harding.[13] At the collinear saddle point, the CH bond distance is 1.58 Å and the CN bond distance is 1.17 Å. Again, the CH bond is greatly extended at the barrier and excitation of the CH stretch will efficiently promote the reaction rate.

As in the HCN(004)/HCN(302) case we measure the ratio of rate constants of the pairs (104)/(402) near 682 nm and (204)/(502) near 600 nm. Surprisingly the (104) and (402) states of HCN react at a similar rate with chlorine atoms: a ratio of $k(104)/k(402) = 1.05 \pm 0.05$ is observed. This finding can be explained by the 3:2 anharmonic resonance (Fermi resonance) between the ν_1 and ν_3 modes.[32,34–37] The (104) and (402) states undergo quite strong anharmonic interaction.[32,34] Assuming that most of the (402)←(000) transition intensity is due to the mixing, from the intensity ratio we obtain the mixing amplitudes 0.73 and 0.69 for the (104) and (402) states, respectively.[34] Thus the vibrational wave functions and thereby the reactivity of HCN in these vibrational states are very similar. To a certain

TABLE II. Ratio of rate constants of the reaction Cl+HCN(ν_1,ν_2,ν_3).

Ratio of rate constants		Dye mixing
k_{004}/k_{104}	1.25±0.4	LDS765/Pyridin 1
k_{005}/k_{104}	5.1 ±0.5	DCM/Pyridin 1
k_{005}/k_{105}	1.05±0.2	R6G/DCM
k_{204}/k_{105}	0.4 ±0.1	R6G/DCM
k_{006}/k_{105}	2.0 ±0.3	Fluorescein 27/R6G

extent this is also the case for the (204)/(502) pair, where the (204) level of HCN is in Fermi resonance with the (502) level. However, the anharmonic mixing is weaker, and the mixing amplitudes are calculated to be 0.9 and 0.44 for the (204) and for the (502) states, respectively. Consequently, we have measured different rate constants between the reactions HCN(204)+Cl and HCN(502)+Cl. Since we could not determine the CN state distributions from both reactions we assume in Eq. (3) $P_{204}\approx P_{502}$ and a ratio of rate constants of $k(204)/k(502)=1.2\pm0.1$ is determined. Again, the (204) state of HCN promotes the Cl+HCN reaction more efficiently than that state having the main part of its energy in the CN stretch. The weakest mixing occurs for the (004) and (302) states of HCN and therefore, the corresponding rates with chlorine differ most.

To compare the reaction rates between vibrational states of HCN which are not energetically close together, we tuned the excitation laser alternately on a known rotational transition of the two vibrational bands. The required wavelength region of the dye laser was obtained by mixing different dyes together. The results are listed in Table II. In order to determine the ratio of rate constants between the states (204) and (105) according to Eq. (3) we assume that $P_{204}/P_{105}\approx P_{104}/P_{005}$. This assumption seems to be valid from the observed CN product state distributions generated in other HCN(ν_1,ν_2,ν_3,J) reactions.

Figure 2 shows all the relative rates as a function of internal vibrational energy. The relative rate measurements clearly demonstrate the mode selectivity in promoting reactions by vibrational excitation. The CH stretch mode ν_3 promotes the Cl+HCN reaction much more efficiently than the CN stretch mode ν_1. The (005) state reacts four times faster, the (006) state even eight times faster than the (004) state of HCN. This is not surprising, because the CH bond is the one which has to break. The reaction rate of Cl+HCN(006) is already close to the gas kinetic limit which was roughly estimated by comparing the intensity of the signal with the sensitivity of the apparatus known from various dissociation experiments.[38]

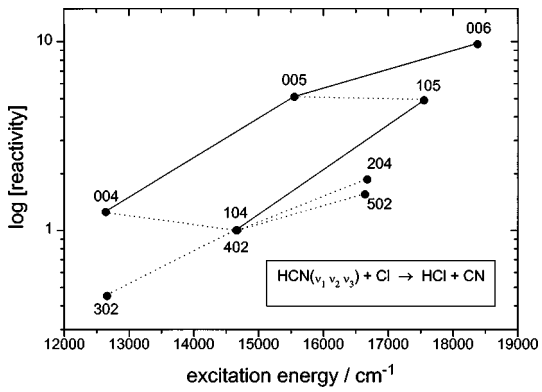

FIG. 2. Reactivity for the Cl+HCN reaction as a function of the excitation energy of HCN.

An additional excitation of the CN stretch does not change this behavior. The reaction of chlorine atoms with HCN is five times faster when HCN is excited to the (105) state instead of the (104) state. The reaction of HCN molecules excited to nearly isoenergetic states that correspond to different nuclear motions provides further evidence that the unreacting bond is a spectator in the reaction. Channeling vibrational energy into a coordinate perpendicular to the reaction coordinate by exciting the CN stretch will have only a minor influence on the reactivity. The observed mode selectivity (isoenergetic states with different nuclear motions have unequal reaction rates) demonstrates that the reaction must be fast where the time left is not sufficient for energy redistribution. Thus we expect the H/Cl+HCN reaction to be a direct abstraction reaction leaving the unreacted CN bond largely with its initial vibrational excitation.

A small influence of the CN stretch can be seen in Fig. 2 by comparing the relative rates of the HCN(ν_1,0,4)+Cl reaction with $\nu_1=0$, 1, and 2. The observed increase of reactivity reflects the properties of the normal-mode model of HCN, which accurately describes the highly excited stretching vibrations in HCN.[39] A single excitation of one of the two stretch modes of HCN corresponds to nuclear motions in both the CH and the CN bonds. Consequently, an excitation of the CN stretch causes a weak vibration in the CH bond and thus an increase of reactivity.

Similar mode specific reaction dynamics were observed by Crim *et al.*[40,41] in the reaction of water molecules with Cl and H atoms. They found that the local mode stretching state $|03\rangle^-$ promotes the H+H_2O as well as the Cl+H_2O reaction much more efficiently than the state $|02\rangle^-|2\rangle$ having part of its energy in bending excitation. Furthermore, the H+H_2O reaction is slower when H_2O is excited to the $|12\rangle^-$ vibrational state, which has its excitation energy distributed over both OH stretches and only two quanta are available along the reaction coordinate, even though the energy of the $|12\rangle^-$ level is slightly higher than that of $|03\rangle^-$. These results were explained by a simple spectator model in which excitation in the nonreacting OH bond is inefficient in promoting the reaction.

B. The role of reactant rotational excitation on the reactivity

Because the line intensities in action spectra depend on both the absorption cross section and the reaction probability, one can measure the reaction rate not only in dependence on the vibrational state, but also on the rotational state of HCN. We have studied the influence of highly rotationally excited HCN on the reaction rate of the reaction

$$\mathrm{HCN}(\nu_3=4,J)+\mathrm{Cl}\rightarrow\mathrm{HCl}+\mathrm{CN} \tag{4}$$

by measuring an action spectrum of the $(\nu_3=0,J)\rightarrow(\nu_3=4,J'=J-1)$ in the wavelength region 793.5–799 nm.

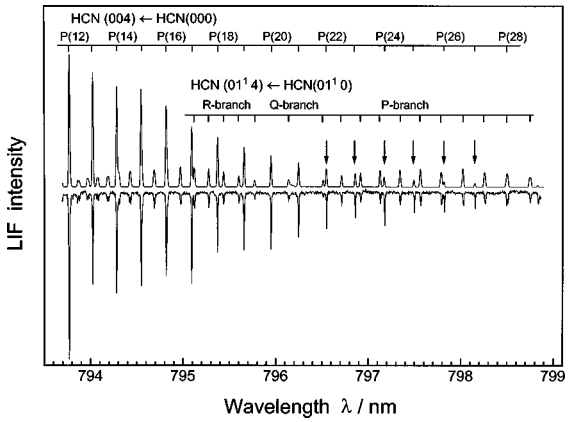

FIG. 3. Action spectrum (lower part) and simulation (upper part) for the Cl+HCN(004) reaction. The intensities of rotational lines belonging to high rotational states with $J'>21$, marked by arrows, are higher in the action spectrum than in the simulation.

Figure 3 shows the CN fluorescence signal (lower part) as a function of the excitation wavelength. Because the signals of the high rotational transitions are very weak, the action spectrum could only be measured at higher pressures and delay times. At a total pressure in the reaction cell of 900 mTorr and a time delay of 300 ns, the HCN molecules have about 3 to 4 collisions prior to the CN detection. Thus partial rotational relaxation might have occurred. By comparing the line intensities of each rotational transition with those from the simulation (upper part in Fig. 3), we obtain the information on the relative reactivity of an individual rotational state of HCN. The dependence of the reactivity on the rotational quantum number J' is shown in Fig. 4. While the reaction rate for $J'<16$ is not affected by rotation, we found an increase of the reactivity for higher rotational levels. HCN molecules in the ($\nu_3=4$, $J'=28$) state react about three times faster than those HCN molecules in the ($\nu_3=4$, $J'<16$) states. Thus high rotational excitation of the HCN molecules can efficiently promote the reaction rate with chlorine atoms.

We assume that this effect is not due to the increase of the total internal energy in HCN when exciting high rotational levels. The difference of rotational energies between $J'=16$ and of the $J'=28$, $E_{\mathrm{rot}}(28)-E_{\mathrm{rot}}(16)=720\ \mathrm{cm}^{-1}$, is much less than the vibrational energy of one CH stretch quantum ($E_{\mathrm{vib}}=3311\ \mathrm{cm}^{-1}$).

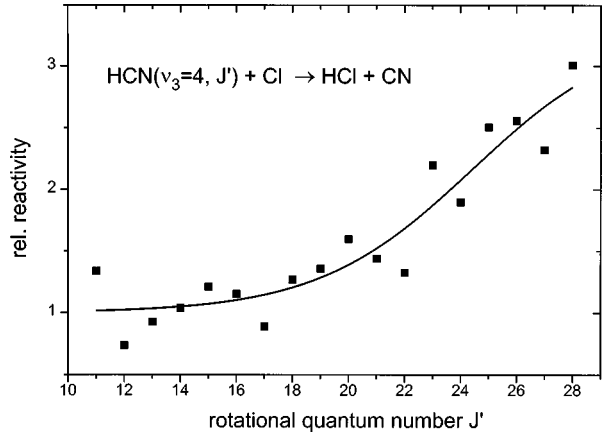

FIG. 4. Relative rate of the Cl+HCN($\nu_3=4,J'$) reaction as a function of the rotational quantum number J'. The reactivity increases with increasing rotational excitation of HCN.

The increase of reactivity is rather a consequence of a geometrical constraint of the Cl+HCN reaction. In Sec. III D we will present measurements of the reaction rate for two different alignments of the reactants. The observed steric effect was explained by a favored reaction geometry where the Cl atom reacts with the H atom end of HCN. When the rotation of HCN is low compared to the passing time of the Cl atom, the reaction can occur only if the Cl atom approaches on the H atom end of HCN. However, at fast rotations of HCN, when the time of rotation is faster than the passing time, the Cl atom has enough time to find the ideal approach geometry.

In order to estimate the typical passing time T_p, we assume a maximum distance of intermolecular forces between Cl and HCN of $d=4$ Å (gas kinetic diameter). With a thermal relative velocity of

$$\nu_{\mathrm{rel}}=\sqrt{2E_{\mathrm{coll}}/\mu}=685\ \ \mathrm{m/s} \tag{5}$$

we obtain a mean passing time of $T_p=d/\nu_{\mathrm{rel}}=0.6$ ps. The time of rotation, $T_r=2\pi/\omega$, is given by the rotational energy

$$E_r=\frac{1}{2}\,I\cdot\omega^2=\frac{1}{2}\,\frac{\hbar}{4\pi c_0 B}\cdot\omega^2. \tag{6}$$

The energy of a rotational state with the quantum number J is given by

$$E_r=2\pi\hbar c_0 B\cdot J'(J'+1)\approx 2\pi\hbar c_0 B\cdot J'^2. \tag{7}$$

From Eqs. (6) and (7) we finally obtain the time of rotation

$$T_r=(2\cdot c_0\cdot B\cdot J')^{-1}=11.6\ \ \mathrm{ps}/J'. \tag{8}$$

For HCN in the $J'=8$ level we obtain $T_r=1.5$ ps, which is slower than the passing time T_p. Thus the chlorine atom passes the HCN molecule, which apparently is not moving. For higher rotational levels with $J'>19$ the situation changes: For example, the time of rotation for HCN in the $J'=28$ rotational level is $T_r=0.4$ ps, which is shorter than the typical passing time.

On the other hand, in the region $0<J'<26$ the reactivity of the reaction HCN($\nu_3=5$, J')+Cl→HCl+CN is independent from J'. We believe that the reaction rate cannot be further enhanced by rotational excitation because the reaction of HCN in the highly vibrationally excited state with $\nu_3=5$ is already very fast [In Sec. III A we obtained $k(005)/k(004)\approx 4$.] Neither did we observe an effect in the reaction of fast H atoms with HCN($\nu_3=4$). Because of the high relative velocity of about 12 900 m/s we obtain an extremely short passing time, $T_p=25$ fs. Thus for all observed rotational levels we have $T_p \ll T_r$.

For an attractive potential the speed of the approaching reactants will be accelerated. Therefore the passing time might be slightly less than one calculated from thermal velocities. Nevertheless, the order of magnitude of the passing time will remain unchanged.

We have already mentioned that the action spectrum shown in Fig. 3 was not measured under nascent conditions

TABLE III. CN product state distributions from different Cl+HCN reactions. The vibrational distributions have an uncertainty of about ± 0.03 for $v=0$, 1, and $v=2$. E_{av} is the available energy equal to $E_{coll}+E_{int}-\Delta_r H^0$. E_{int} is the internal vibrational and rotational energy of HCN equal to $E_{int}=E_{vib}+BJ'(J'+1)$, $J'=9$. E_{rot} and E_{vib} are the rotational and vibrational energies of the CN product.

Experiment	E_{coll}[b,c]	E_{int}[b]	E_{av}[b]	$v=0$	T_{rot}/K	$v=1$	T_{rot}/K	$v=2$	T_{rot}/K	$v=3$	T_{rot}/K	E_{rot}[b]	E_{vib}[b]
Cl+HCN(002)	36	79	21	0.86	1700±45	0.13	940±50	<0.01	···	···	···	13.3	3.7
Cl+HCN(004)[a]	36	152	94	0.51	910±50	0.34	840±40	0.15	740±40	···	···	7.2	15.6
Cl+HCN(004)	25	152	83	0.52	900±60	0.34	820±50	0.14	820±160	<0.02	···	7.2	15.3
Cl+HCN(302)	25	152	83	0.45	820±60	0.43	760±50	0.12	660±130	<0.02	···	6.5	16.3
Cl+HCN(402)	25	177	108	0.68	730±50	0.25	750±50	0.07	620±50	<0.02	···	6.0	9.7
Cl+HCN(104)	25	177	108	0.71	730±50	0.23	710±50	0.06	700±50	<0.02	···	6.0	8.4
Cl+HCN(005)	25	186	117	0.41	710±50	0.38	750±50	0.15	720±50	0.06	530±50	5.8	21.4
Cl+HCN(105)	25	211	142	0.65	730±23	0.25	700±70	0.10	640±60	<0.02	···	6.0	11.0
Cl+HCN(006)	25	221	152	0.34	740±30	0.34	610±30	0.23	690±60	0.09	660±60	5.6	26.0

[a]Reference 21.
[b]Energies in kJ/mol.
[c]E_{coll} is the average of a distribution of collisional energies. From Ref. 21.

($P\cdot\tau=0.27$ Torr μs). Thus the initial preparation of HCN in a specific rotational state was scrambled by nonreactive collisions in the time scale of the measurements. *R-R* energy transfer is the primary relaxation pathway for rotationally excited molecules in our experiment. There are no data for rotational relaxation of HCN out of the (004) levels, but measurements for the (003) levels[42] allow an estimation of the rotational relaxation. Wu *et al.*[42] found that the relaxation rate of rotational levels with $5<J'<15$ are at least $k_{R\text{-}R}=150$ Torr^{-1} μs^{-1}. Thus the relaxation time is $0.27\cdot 150\approx 40$ times faster than our time delay. The relaxation of rotational levels with $J'>25$ proceeds slower with a relaxation rate of $k_{R\text{-}R}<10$ Torr^{-1} μs^{-1}. This means that complete rotational relaxation will have occurred only in low lying rotational levels. On the other hand, most of the HCN molecules in high rotational levels did remain in the initially prepared rotational state or in states close to it. Consequently, the effect of rotational relaxation in high rotational levels was small.

C. Influence of the initial HCN excitation on the CN product state distribution

The complete CN product state distribution is obtained by probing the rovibrational transitions of the $B\,^2\Sigma^+ \leftarrow X\,^2\Sigma^+$ system. Simulations of the CN spectrum were used to fit all observed rotational lines. We have already reported the product state distribution of CN in the reaction of chlorine atoms with HCN(002), HCN(004), HCN(302), and HCN(105).[21] In this paper we will continue the investigation by analyzing the reactions of Cl atoms with HCN(104), HCN(402), HCN(005), and HCN(006). The characteristic quantities of all CN product state distributions are listed in Table III. The main result is that the amount of vibrational excitation in the CN product depends strongly on the initially prepared vibrational state of HCN. First, we find that the CN vibration increases linearly with increasing pure CH-stretch excitation. The reaction of Cl with HCN($\nu_3=2$) leads to less vibrationally excited CN products with population ratios of $P(v=0):P(v=1):P(v=2)=86\%:13\%:<1\%$, while the reaction of Cl with HCN($\nu_3=4$) leads to CN products with 52% in $v=0$, 34% in $v=1$, and 14% in $v=2$. Highly vibrationally excited CN products are obtained when Cl reacts with HCN where 6 CH stretch quanta are excited (Fig. 5, lower part). Second, we find a mode-specific dependence of the CN vibrational excitation. In contrast to the reactions of HCN where only the CH stretch mode is excited, an additional excitation of one CN stretch quantum surprisingly leads to a decrease of CN vibrational excitation. A fit of the spectrum when highly excited HCN(104) is used as reactant yields that 71% of the CN radicals are generated in $v=0$, 23% in $v=1$, and 6% in $v=2$. Although the excitation energy of the (104) state is higher than that of the (004) state, we obtained a significant change in the former tendency of increasing CN vibration with increasing CH stretch excitation. The CN vibrational excitation decreases again, although one quantum of CN stretch has been excited in addition to four CH stretch quanta. The same situation was found when HCN was prepared in a state having five quanta of CH stretch and one quanta of CH stretch excitation (Fig. 5, upper part). The reaction leads to CN where only 35% of all molecules are in vibrationally excited states ($v>0$), compared to 59% when

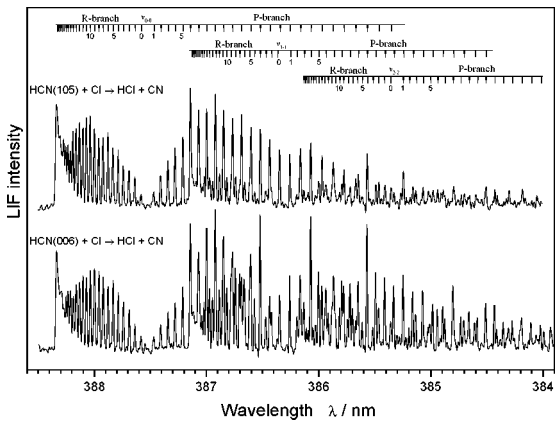

FIG. 5. Laser-induced fluorescence spectra of CN generated in the reactions of chlorine atoms with HCN in the (105) state (upper part) and in the (006) state (lower part). The reactions lead to different CN product state distributions.

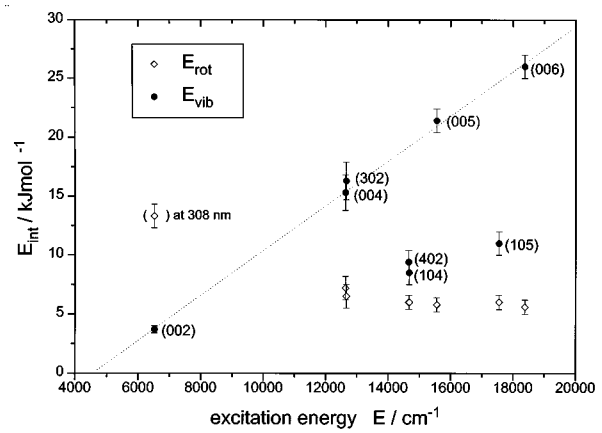

FIG. 6. Vibrational and rotational energy of the CN product as a function of the HCN excitation energy. The chlorine atoms in the Cl+HCN(002) reaction are generated from the photolysis of Cl_2 at 308 nm. The vibrational energy of CN from the reaction of Cl with HCN$(00\nu_3)$, $\nu_3=2-6$, can be fitted by a straight line.

HCN is excited to the (005) state. The additional excitation of one quantum of CN stretch does not increase the vibration of the CN product.

On the other hand, the state distributions of CN are similar when HCN is excited to the isoenergetic states (004) and (302). The CN vibrational energy in the reactions HCN(004)+Cl and HCN(302)+Cl are 15.5 and 16.3 kJ/mol, respectively (Table III). Further on, we find a similar vibrational energy release in the CN product when HCN is excited to the isoenergetic (104) and (402) states (8.4 and 9.7 kJ/mol, respectively). We believe that the 3:2 anharmonic resonance is responsible for an increased complexity of our state selective data. The two states (104) and (402) that undergo the strongest anharmonic interaction lead to CN products with vibrational energies differing only by 15%. For the last resonant pairs (205)+(502) we could not measure nascent CN spectra in order to compare the CN state distribution.

The mode specific dependence of the CN vibrational excitation is illustrated in Fig. 6 where the internal CN energies (vibration and rotation) are depicted as a function of the HCN excitation energy. First of all, it is surprising that the CN vibration increases with increasing CH stretch excitation. As we can see in Fig. 6 the vibrational energy increases almost linearly with the excitation energy of the HCN$(00\nu_3)$ states with $\nu_3=2$, 4, 5, and 6. We believe that the observed increase of the product vibrational energy is due to the normal-mode model of the initially prepared vibrational states of HCN. As we have described in Sec. III A, after exciting the pure CH stretch mode of HCN, not only the CH bond, but also the CN bond is in motion. If the reaction is direct (e.g., stripping reaction) and the initial motion in the CN bond is transferred into the CN product, an excitation of the CH stretch causes a weak vibrational excitation of the CN product. A qualitative quantum mechanical explanation could be as follows. Figure 7 shows various wave functions for HCN as functions of the internal bond distances (adapted from Ref. 43). The dashed line indicates the bond length of the free CN radical. In the case of the $(00\nu_3)$ states of HCN, the CN distance decreases with increasing CH distance. One can assume that the reaction only occurs if the CH bond is lengthened, i.e., at the upper left corner of the probability density diagram of Figs. 7(a) and 7(b), where the probability is highest (classical turning points), because the high-energy eigenstates are strongly anharmonic. Since the CN bond is compressed at the turning point, at the end of the reaction the CN molecule will be vibrationally excited. The observed variation of the product state distribution when exciting an additional quantum of CN stretch reflects the properties of the vibrational wave functions of HCN, too. Figures 7(c) and 7(d) show the wave functions for HCN in the states (104) and (105). Because the vibrational quantum number ν_1 is now equal to one, the two states have a regular structure with an additional node along the second stretch coordinate. In contrast to the case discussed above, the end peak with the largest CH bond distance has now a CN bond distance close to the equilibrium distance of the free CN molecule. If the reaction proceeds via a direct stripping mechanism, then the CN product should not be vibrationally excited which is exactly what was observed in our experiments. This assumption agrees with the qualitative spectator model from Sec. III A, because the CN product vibrational excitation directly reflects the nodal pattern of the vibrational wave function in the excited HCN molecule. However, it should be mentioned that this simple model neglects any influence of the approaching Cl atom on the Cl–H–CN coordinates of the potential-energy surface.

The vibrational excitation of the CN molecule seems to be a consequence of the initial vibration of HCN. This assumption is also confirmed by the results of the H+HCN reaction (2).[21] Figure 8 illustrates this by comparing the state distributions of the CN fragment from both the chlorine and the hydrogen reaction. Both reactions produce CN with a very similar vibrational distribution, suggesting that the vibrational state distribution is not determined by mass effects.

With respect to our interpretation it is important to point out that the eigenstates of HCN, depicted in Fig. 7, are only correct for the free molecule. They are more complicated when the Cl atom approaches the HCN molecule. Thus exact explanations can only be made with quantum mechanical calculations of the complete four-atom system Cl+HCN.

The main result concerning the rotational distribution of CN is that each distribution can be well characterized by rotational temperatures. In general, the CN products from the reaction of Cl with vibrationally excited HCN are rotationally cold (Table III). The only exception is the reaction Cl+HCN(002)→HCl+CN which produces CN products with the characteristic temperature parameters of $T(v=0)=1700$ K and $T(v=1)=945$ K.[21] The rotational energy of the CN products slightly decreases with increasing HCN excitation (see Fig. 6). The lowest rotational excitation of CN from the reaction with Cl is obtained for HCN(006), where the CN product receives only 4% of the energy available to the reaction ($E_{\mathrm{rot}}=5.6$ kJ/mol). Even less rotational excitation of CN is obtained from the reaction of hydrogen atoms with HCN(002) and HCN(004)[21] (Fig. 8). At a collision energy of 80 kJ/mol, only 4.5 kJ/mol (002) and 3.8 kJ/mol (004) remain in the CN product rotation.

Since the temperatures of the experimental CN rotational

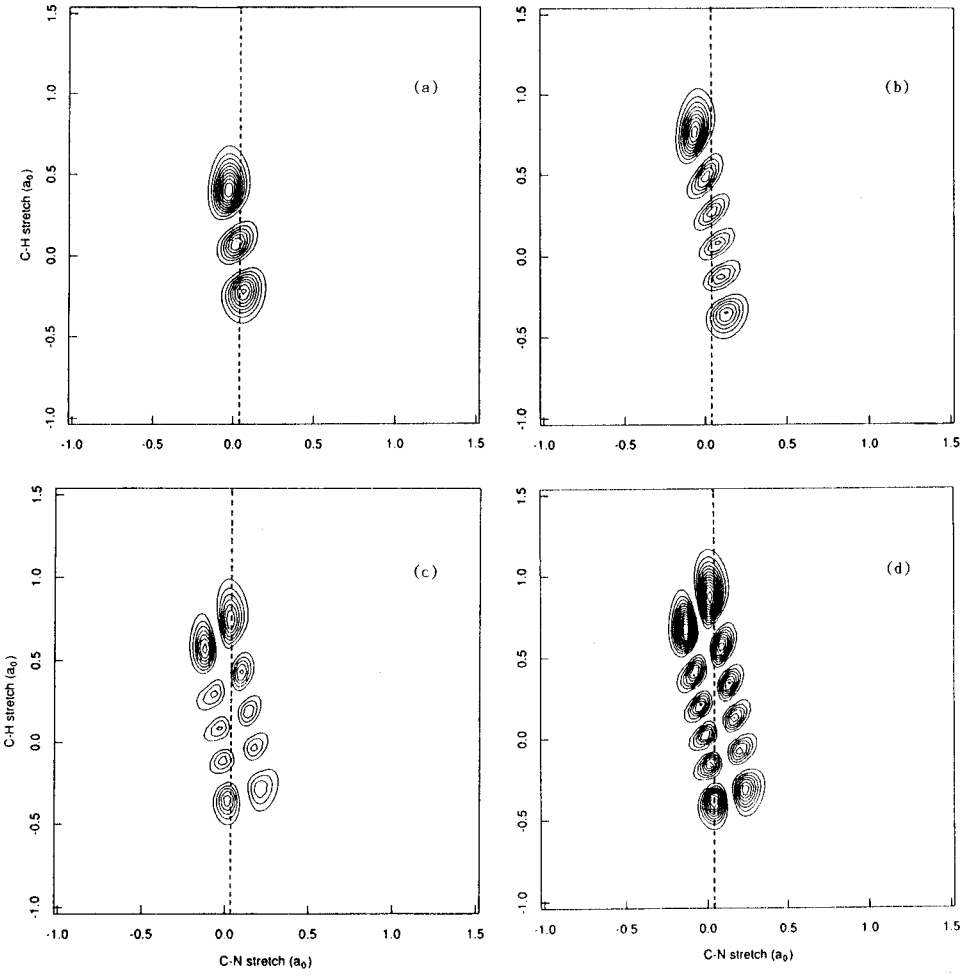

FIG. 7. Ψ^2 contour plots of the wave function of some HCN overtones, adapted from Ref. 43. The wave functions are easily identified by counting the nodal planes; (a) 002; (b) 005; (c) 104; and (d) 105. The dashed line indicates the bond length of the free CN radical.

distributions for the H/Cl+HCN reactions are low, we assume that both reactions produce CN mainly by direct mechanisms with a collinear transition state. This result agrees well with theoretical results by Clary.[44]

The cause for the rotational excitation of the CN product from the reaction $H+HCN \rightarrow H_2+CN$ are manifold. Rotational excitations may result from the zero-point energy of the bending mode of HCN, from their cone of acceptance for the H atom (large orbital angular momentum) or from the initial rotation of the HCN molecule. To examine the role of the initial HCN rotation on the CN product rotation we prepared the HCN molecule in different rotational levels of the (004) vibrational state. The rotational distribution of CN($v=0$) was obtained by probing the P branch of the ($v'=0 \leftarrow v=0$) transition in the wavelength region of 388.5–387.5 nm. We prepared the HCN molecule in rotational states with rotational quantum numbers of $J'=2$, 9, and 16. All rotational distributions are well characterized by Boltzmann distributions and the respective temperatures for CN($v=0$) are 490 K±7%, 530 K±5%, and 620 K±4%. The rotational excitation of the CN product increases with increasing rotational excitation of the HCN product. Therefore we observe a positive correlation between reactant and product rotation.

D. Influence of the collision energy on the CN product state distribution

In order to study the influence of the collision energy on the product state distribution a shorter photolysis wavelength was used. When Cl_2 is photodissociated at 308 nm instead of 355 nm, the collision energy of the system Cl/HCN increases by 11 kJ/mol from 25 to 36 kJ/mol.[21] However, this increase in collision energy has no significant effect on the CN product state distribution (see Table III). This is also confirmed by the study of Crim and co-workers who used thermal Cl atoms ($E_{coll}=4$ kJ/mol) to study the reaction with HCN(004) leading to the same CN product state distribution as in the present experiment. Therefore the Cl+HCN(004) reaction generates CN products with the same amount of vibrational energy over a wide range of collisional energies. Therefore the translational energy of the reactants is not responsible for the vibrational excitation of the CN product as an impulsive model would suggest. It is rather due to the initial vibrational excitation of the HCN molecule (Sec. III C).

Likewise, no significant effect of the collision energy on the observed vibrational distribution of CN was found for the hydrogen reaction (2). The reactions of HCN($\nu_3=4$) with thermal H atoms ($E_{coll}=4$ kJ/mol) and photolytic H atoms

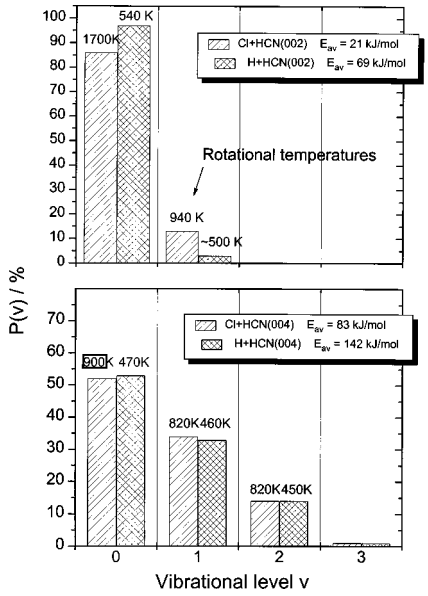

FIG. 8. Vibrational state distribution and rotational temperatures of CN produced in the reactions of H and Cl atoms with vibrationally excited HCN($00\nu_3$).

(E_{coll}=80 kJ/mol) lead to very similar vibrational distributions of the CN product: The CN vibrational energies are 12.7 and 14.9 kJ/mol, respectively. Again, the vibrational excitation of CN cannot be a consequence of using fast H atoms with high translational energy. Therefore one would predict a low product vibrational excitation of the CN fragment when fast hydrogen atoms react with HCN in the vibrational ground state. This assumption was confirmed by Lambert *et al.*[45] and Johnston *et al.*[46] who observed a CN state distribution which is characterized by a relatively high rotational and low vibrational energy release, similar to the Cl+HCN(002) reaction (Table III).

E. Stereospecific reaction dynamics

In order to study the steric effect in the reactions of H+HCN(ν_3=2,4)→H_2+CN and Cl+HCN(ν_3=2,4)→HCl+CN, the reactants were optically aligned using linearly polarized laser light. All relative rate measurements were performed for two different reactant approach geometries by rotating the polarization vector $\vec{E}_{exc}$ of the HCN excitation laser beam with respect to the vector $\vec{E}_{phot}$ of the photolysis laser beam.

The fragments of the photodissociation show an anisotropic distribution of recoil velocities, which has an expression of the form

$$P(\vartheta)=[1+\beta\cdot P_2(\cos\vartheta)]/4\pi. \tag{9}$$

$P(\vartheta)$ is the probability to realize a certain angle ϑ, which is the angle between the polarization vector $\vec{E}$ and the direction of the velocity of the photofragment. $P_2(\cos\vartheta)$ is the second Legendre polynomial, and the so-called ''β parameter'' provides a quantitative measure of the recoil anisotropy.[47] The parameter range varies from +2 for a pure $\cos^2\vartheta$ distribution to −1 for a pure $\sin^2\vartheta$ distribution. For β=0, the distribution is isotropic. The chlorine atoms from the photolysis

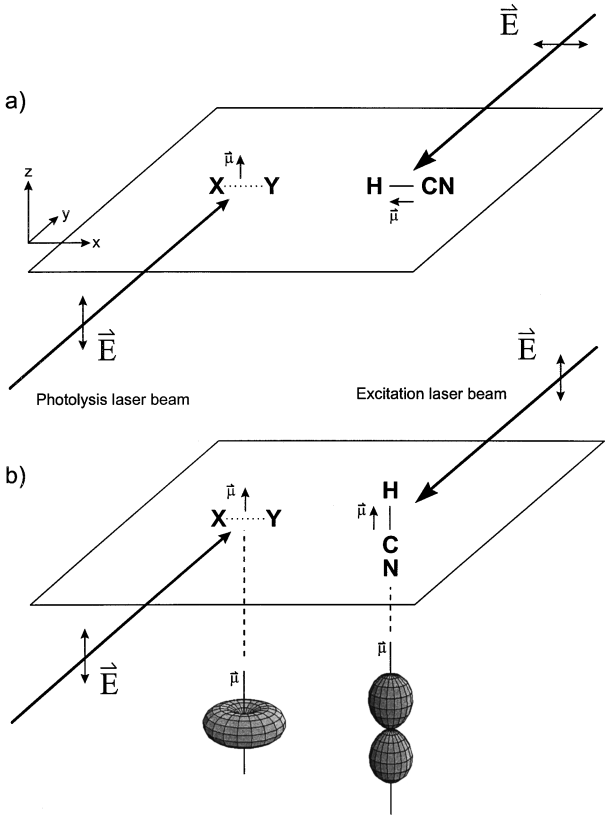

FIG. 9. Schematic view of the two approach geometries after preparation of the reactants with linearly polarized light. (a) $\vec{E}_{exc}\perp\vec{E}_{phot}$ and (b) $\vec{E}_{exc}\|\vec{E}_{phot}$.

of Cl_2 at 355 nm as well as the hydrogen atoms from the photolysis of methanethiol at 266 nm show an angular distribution, which is described by an anisotropy parameter of $\beta=-1$ (see Sec. II). Thus the photolysis is a prompt dissociation following excitation via a transition dipole moment μ which lies perpendicular to the molecular bond. Thus the angular distributions of the hydrogen and chlorine atoms nearly have a $\sin^2\vartheta$ distribution and the most probable flight path lies in the xy plane (Fig. 9).

The transition dipole moment of the HCN $^1\Sigma-^1\Sigma$ transition lies along the intermolecular axis of the molecule. Thus the linearly polarized laser beam selects HCN molecules whose intermolecular axes have an initial distribution of $\cos^2\theta$, where θ is the angle between μ and $\vec{E}_{exc}$ (Fig. 9). Because the HCN molecule rotates prior to collision, the degree of alignment depends strongly on the rotational state of HCN. The exact quantitative expressions for this alignment are described by Zare.[48]

In a forthcoming paper[49] equations are developed which allow a relatively easy conversion of experimental results to the angle of attack. A qualitative understanding of the influence of polarized light on the preferred reaction geometry can be extracted from Fig. 9 which shows the approach geometry of the reactants if the polarization vector $\vec{E}_{exc}$ of the HCN excitation laser beam is perpendicular [Fig. 9(a)] or parallel [Fig. 9(b)] to the polarization vector $\vec{E}_{phot}$ of the photolysis laser beam. In the first case ($\vec{E}_{exc}\perp\vec{E}_{phot}$), the favored approach geometry for the photolysis fragments is

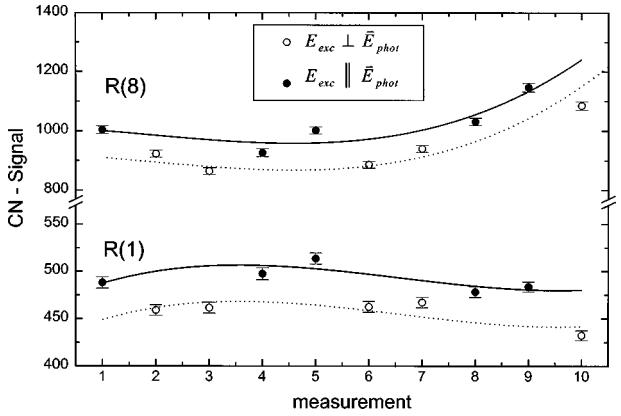

FIG. 10. Relative reactivity of the H+HCN($\nu_3=4,J$)→H_2+CN system measured in alternating order of the two approach geometries. The HCN molecule is excited to the vibrational state via the $R(1)$ and the $R(8)$ rotational transitions. Solid circles mark the relative rates with the polarization vectors aligned perpendicular to each other, while open circles mark the rates with the polarization vectors aligned parallel to each other.

both end-on and side-on with respect to the HCN molecule. In the second case ($\vec{E}_{\mathrm{exc}} \| \vec{E}_{\mathrm{phot}}$), the fragments preferentially approach the broadside of HCN (side-on). The rotation of the polarization plane of the excitation laser beam was simply achieved by a $\lambda/2$ plate which was mounted in front of the entrance window of the reaction chamber.

To determine the effect of molecular alignment on the reactivity we tuned the probe laser to the $R(8)$ rotational line of CN($v=0$) and measured the laser-induced fluorescence intensity for the perpendicular and the parallel case. Mean CN signals of one reaction geometry were obtained by summing up over 400 single measurements. This was repeated several times with altering approach geometry. The result for the H+HCN($\nu_3=4,J$)→H_2+CN reaction is shown in Fig. 10. The HCN molecule was excited to the vibrational state via the $R(1)$ and the $R(8)$ rotational transitions. The time delay between the excitation/photolysis laser and the probe laser was 230 ns, at a total pressure in the reaction cell of 500 mTorr. Figure 10 clearly shows that the signal intensity is higher for the perpendicular case than for the parallel case. The signals are used to calculate the alignment effects defined by

$$S = I_{\perp}/I_{\parallel}. \tag{10}$$

We obtain a small but significant alignment effect of $S=1.07\pm0.03$ for the $R(1)$ and 1.09 ± 0.03 for the $R(8)$ rotational line of HCN. A value of $S>1$ indicates a preference of the approach geometry, where the atoms preferentially attack the HCN molecule end-on. Thus the production of CN is enhanced for collinear collisions of the reactants. A similar result is obtained for the reaction of H atoms with HCN($\nu_2=2$), having an alignment effect of $S=1.12$.

In the same way we measured the steric effect for the chlorine reaction (1). HCN was excited via the $R(8)$ rotational line to the (002) and (004) vibrational levels. Interestingly, we find a mode-specific dependence of the alignment effect S. If HCN is excited to the (002) state we measured a significant preference for the perpendicular case, indicating that the reaction HCN($\nu_3=2$)+Cl proceeds via a collinear transition state. However, a further increase of ν_3 excitation leads to an alignment effect which is close to $S=1.0$. Thus the reaction of Cl with HCN(004) favors an approach geometry, where the angle of acceptance has increased and the Cl atom may also attack the HCN molecule broadside. This observation can be explained by the cone-of-acceptance model for the reaction Cl+HCN.[49] For low vibrational excitation of HCN, only a narrow range of Cl atom approach angles can lead to a reaction. An increase of vibrational excitation widens the cone of acceptance, so that the chlorine atoms can strike the HCN at larger angles. The restriction to a collinear reaction geometry is less if the CH bond in HCN is vibrationally excited. As a consequence the reaction probability increases, while the alignment effect S decreases. Furthermore, the cone of acceptance is larger for the bulky Cl atoms than for the H atoms. Similar results were found by Loesch *et al.*[50,51] in the reaction of Li/K+HF. They found a decrease of the alignment effect, when the bulky K atom reacts instead of Li. This gives evidence that the size of the reacting atom may have an influence on the PES in the region of the transition state and hence, on the cone of acceptance. But this assumption has to be confirmed by quantum mechanical or quasiclassical trajectory studies (QTC). We will present a more general and quantitative description of the different approach geometry and the cone-of-acceptance model in a separate paper.[49]

F. RRKM calculation

We calculated the vibrational population of CN with a simple extension of the Rice–Ramsperger–Kassel–Marcus (RRKM) theory where one assumes that the CN stretch vibration of the transition state migrates adiabatically into vibration of the CN radical. Using this assumption one yields for the vibrational population of the CN product

$$P(v) = \frac{k(v)}{k(E)},$$

where $k(E)$ is the RRKM rate and $k(v)$ is the RRKM rate with a vibrational quantum number of v in the transition state. The proposed reaction pathways and geometries of the transition states are shown in Fig. 11. The used constants for HHCN and ClHCN are listed in Table IV.

The results of the RRKM calculation are listed in Table V. As can be seen, both the Cl+HCN and the H+HCN reaction should generate less vibrationally excited CN products than are observed in the experiment. Therefore RRKM theory is not appropriate to describe the H/Cl+HCN →HCl/H_2+CN reaction. So we conclude that there is not enough time for energy randomization. Both reactions seem to proceed rather direct.

G. Trajectory study

To study the details of how reactant vibrational excitation influences reactivity and product state energy partitioning, we performed quasiclassical trajectory calculations (QTC) for the forward reaction (2). Several quantum theoretical results have been reported concerning the mode-specific reaction rates in H+HCN(ν_1,ν_2,ν_3)→H_2+CN.[52,53]

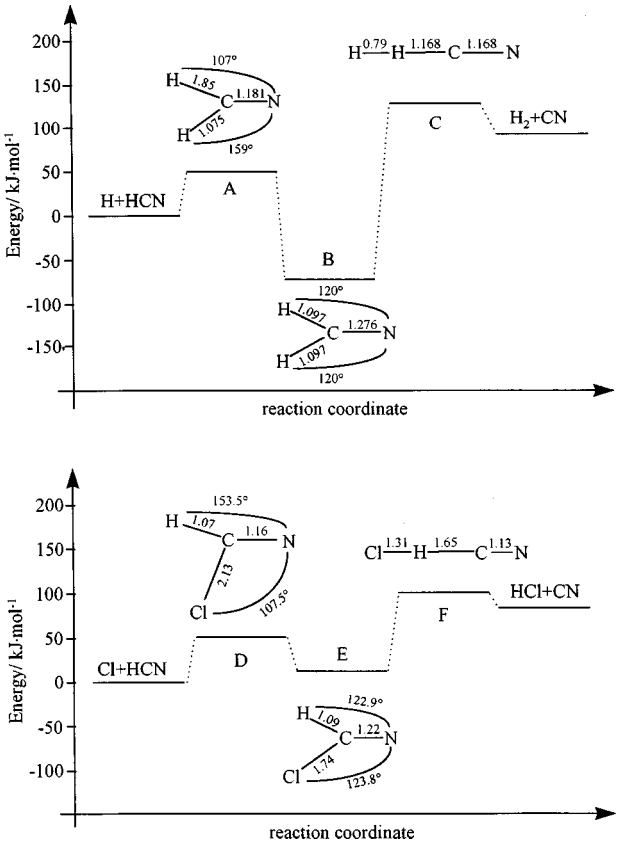

FIG. 11. Reaction geometries and pathways (Refs. 16 and 23) used in the RRKM calculations. Distances are given in Å.

Our trajectories were calculated for a collinear reaction geometry of the four atoms. We used a LEPS-like potential-energy surface (PES) of the form

$$V(r_{H'H},r_{CH'},r_{CH},r_{CN}) = V_{LEPS}(r_{H'H},r_{CH'},r_{CH}) + V_M(r_{CN}), \quad (11)$$

which was developed by Brooks.[54]

Here V_{LEPS} is a three-body LEPS-type surface and V_M is a modified Morse potential to describe the CN interaction. Other PES[55,56] of Sun and Clary do not reproduce the HCN vibrational normal modes with such high accuracy. Using the parameters shown in Table VI the reaction enthalpy of our potential surface is 91 kJ/mol and the classical barrier of the forward reaction is 113 kJ/mol which both are in good agreement with theoretical results. The CH and CN bond distance in the free HCN molecule are 1.00 and 1.17 Å, respectively.

TABLE IV. Constants of the transition states (Refs. 16 and 23).

	A	B	C	D	E	F
ω_1/cm^{-1}	3350	3058	2275	3505	3236	2966
ω_2/cm^{-1}	1950	1761	2110	2375	2104	1821
ω_3/cm^{-1}	1000	1451	771	952	1260	186
ω_4/cm^{-1}	641	1046	213	906	991	88
ω_5/cm^{-1}	844	3130		282	773	
ω_6/cm^{-1}		963			435	
ω_i/cm^{-1}	1303i		1009i	762i		372i
Energy/kJ mol^{-1}	44.77	−79.91	127.61	53.1	17.1	113

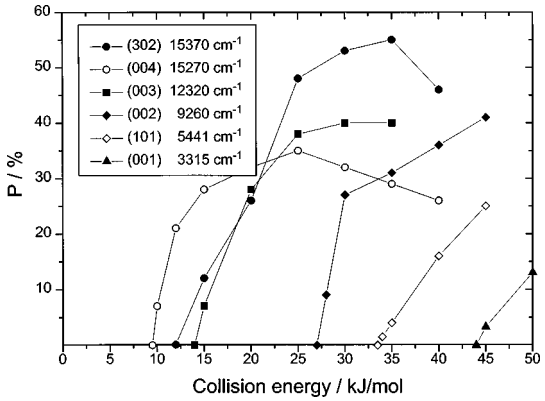

FIG. 12. Reaction probability for H+HCN(ν_1,0,ν_2)→H_2+CN as a function of the collisional energy (in kJ/mol). The reaction probability is equal to the number of trajectories leading to the products divided by the total number of trajectories.

The surface shows a late barrier with bond distances at the saddle point H′HCN of $r_{H'H}=0.85$ Å, $r_{CH}=1.42$ Å, and $r_{CN}=1.165$ Å. The bond distances of the products H_2 and CN are 0.742 and 1.164 Å, respectively. Classical trajectories were obtained using the classical perturbation theory approach for determining good action-angle variables.[57–60] This procedure leads us to specify the initial semiclassical states of HCN accurately.

The total reaction probabilities for H+HCN(001, 002, 003, 004, 101, 302) are plotted in Fig. 11. The results indicate that the reaction threshold is lowered efficiently by vibrational excitation of HCN. This result is consistent with the fact that reaction (1) has a late barrier. More specifically, the threshold is lowered more effectively by exciting the CH stretch than by exciting the CN stretch. While the reaction of HCN in the (001) state occurs at collision energies >44 kJ/mol, no reaction at any collision energy was found if only the CN stretch up to $\nu_1 \leqslant 3$ is excited. The same result was found when HCN is in the vibrational ground state (000). Thus the endothermic reaction with a late barrier cannot be promoted either by translational excitation nor by CN stretch excitation. This is in good agreement to experimental results and theoretical results obtained by Takayanagi and Schatz,[52] who found a very small cross section for the HCN(000)+H reaction at translational energies >110 kJ/mol.

If HCN is excited to different but isoenergetic vibrational states [such as (004) and (302)], the threshold is always lower for the vibrational state where mainly the CH mode is excited. In Fig. 12 it can also be seen that pure CH excitation increases the reaction probability more efficiently than CN excitation. At collision energies lower than 22 kJ/mol the reactivity for HCN(004) is larger than for HCN(302). However, at higher collision energies the reactive rate changes are reversed. This is due to the restriction we have made in the QCT study, namely that the reaction can only proceed via a collinear collision geometry. However, as we have seen from the experiment (Sec. III E), reaction geometries with a wide cone of acceptance can occur. This might also explain why the calculated vibrational CN distributions are higher than the one we measured in the

TABLE V. Results of the RRKM calculations for $R+\mathrm{HCN}(0,0,\nu_3)\rightarrow R\mathrm{H}+\mathrm{CN}(v)$ using the quantities given in Table IV. For a better comparison the experimental results are also listed.

	E_{coll} [kJ/mol]	$v=0$ [%]	$v=1$ [%]	$v=2$ [%]	$v=3$ [%]	$v=4$ [%]	$v=5$ [%]
H+HCN(002)RRKM	80	98	2	0	0	0	0
H+HCN(002)Exp.	80	95	<5	0	0	0	0
H+HCN(003)RRKM	80	84	15	1	0	0	0
H+HCN(004)RRKM	80	69	24	6	1	0	0
H+HCN(004)Exp.	80	53	33	14	0	0	0
H+HCN(005)RRKM	80	60	28	9	2	0.4	0
H+HCN(006)RRKM	80	52	30	12	5	1	0.3
Cl+HCN(002)RRKM	36	100	0	0	0	0	0
Cl+HCN(002)Exp.	36	86	13	<1	0	0	0
Cl+HCN(003)RRKM	25	100	0	0	0	0	0
Cl+HCN(004)RRKM	25	96	4	0	0	0	0
Cl+HCN(004)Exp.	25	51	34	15	0	0	0
Cl+HCN(005)RRKM	25	89	11	0.4	0	0	0
Cl+HCN(005)Exp.	25	41	38	15	6	0	0
Cl+HCN(006)RRKM	25	78	20	2	0.1	0	0
Cl+HCN(006)Exp.	25	34	34	23	<9	0	0

experiment. At a collision energy of $E_{\mathrm{coll}}=80$ kJ/mol the QCT calculation leads to CN vibrational distributions $P(v=0):P(v=1):P(v=2):P(v=3)$ of 0.51:0.39:0.10:0.0 for the HCN(002) reaction and 0.10:0.30:0.23:0.35 for the HCN(004) reaction.

Thus one can assume that the reaction will proceed via the collinear transition state if the collision energy is thermal. Figure 13 shows the result of the trajectory calculation with a Boltzmann-like collisional energy distribution at 300 K which was obtained by arbitrarily choosing a collision energy between 0 and 50 kJ/mol for each trajectory. At the end of the trajectories, the reaction probability is weighted by $P(E_{\mathrm{coll}})=E_{\mathrm{coll}}\cdot\exp(-E_{\mathrm{coll}}/kT)$. This leads to a mean collision energy of 4 kJ/mol. Figure 13 compares the QCT results with our experimental results where thermal hydrogen atoms were used as collision partners. The translational relaxation is achieved by adding He into the reaction cell, as described in Ref. 21. In the upper part of Fig. 13 the CN vibrational distributions are plotted which belong to the $\mathrm{H}+\mathrm{HCN}(\nu_3=2)$ reaction, while in the lower part those which belong to the $\mathrm{H}+\mathrm{HCN}(\nu_3=4)$ reaction are plotted. In both cases there is a very good agreement between the QCT result and the experiment. The calculated rates of reactivity are $k_{003}/k_{002}=34\pm4$, $k_{004}/k_{003}=5.7\pm0.6$, and $k_{004}/k_{302}=3.7\pm0.4$. Thus the reactivity is enhanced by a factor of 194 ± 43 when HCN is excited to the (004) state instead of (002). Furthermore, the reactivity is larger when the vibrational energy is located only in the CH mode, instead of locating the same energy in both CH and CN stretch modes of HCN. Again, the calculated rate k_{004}/k_{302} is in good agreement with the experimental result ($k_{004}/k_{302}\leqslant 4$).[21]

We also calculated the energy release into the vibration of the H_2 product at a thermal collision energy of 4 kJ/mol. When HCN is in the (002) vibrational state, about 12%, 64%, and 24% of the total available energy are located in CN vibration, H_2 vibration, and in product translation, respectively. If HCN is excited to the (004) vibrational state, the energy release was found to be 21%, 61%, and 18%, respectively. Thus about 2/3 of the available energy are located in the H_2 vibration. This result is consistent with theoretical results showing that vibrational excitation of H_2 can efficiently promote the reverse reaction $H_2+CN\rightarrow H+HCN$ and that a significant energy transfer into the vibration of the CN product must occur. The CN internal energy release increases with increasing CH stretch excitation which is also found in the experiment (Sec. III C).

TABLE VI. Parameters used in the potential-energy function (LEPS). Other parameters: $p_{\mathrm{CH}}=-0.136$, $p_{\mathrm{CN}}=-0.059$, and $q=0.75a_0^{-1}$. (1 hartree=219 400 cm^{-1}, $a_0=0.529\,177$ Å).

AB	D_{AB}/hartree	$\beta_{\mathrm{AB}}/a_0^{-1}$	r^0_{AB}/a_0	Δ_{AB}
$H'H$	0.17	1.0583	1.4014	0.1
CH'	0.1528	0.9245	1.9993	0.1
CH	0.2102	0.9245	1.9993	0.1
CN	0.350 59	1.4065	2.1864	-

IV. CONCLUSIONS

We used vibrational overtone excitation to prepare HCN molecules in a specific rotational and vibrational state and to study the influence of reactant excitation on the endothermic reactions $H+HCN\rightarrow H_2+CN$ and $Cl+HCN\rightarrow HCl+CN$. In the reaction of chlorine atoms with HCN, the CH stretch mode promotes reaction much more efficiently than the CN stretch mode. Thus channeling energy into the reaction coordinate will increase the reactivity while energy located in a coordinate perpendicular to the reaction coordinate will have no or only a minor influence on the reaction rate. These results are consistent with the qualitative spectator model in which excitation in the nonreacting CN bond has no effect on the reactivity. The reactions of chlorine atoms with HCN in vibrational states having similar energy but corresponding to very different nuclear motions demonstrate the mode specific behavior of the reactivity. The results agree with a

simple, direct reaction mechanism without complex formation. The reaction must be fast without time left for energy redistribution.

Furthermore, the product vibrational energy is strongly influenced by the initial vibrational state of HCN. The vibrational energy of the CN product distribution in the chlorine reaction could qualitatively be explained by the nodal pattern of the vibrational wave function of the HCN molecule. Hence the CN product vibration is a consequence of the initial vibrational excitation of the HCN molecule. This is again in accordance with the spectator model in which the nonreacting CN bond does not participate in the reaction and is confirmed by the observation that neither different collisional energies of the reactants nor different masses of the reacting atom (H/Cl) have a significant influence on the vibrational distribution of CN.

Reactions from different rotational states of HCN($\nu_3 = 4$) show the influence of an initial rotation of HCN on the reaction. The rotational excitation of HCN promotes the Cl+HCN reaction very efficiently, suggesting a geometrical constraint on the reaction. At low rotations of HCN, the reaction can occur only if the Cl atom approaches on the H atom end of HCN, whereas at fast rotations of HCN, the Cl atom has sufficient time to find the ideal approach geometry. These observations suggest that the relative orientation of the reactants strongly affects the reaction rate, which is confirmed by our measurements with optically aligned reactants. In the case of H+HCN and Cl+HCN the CN is predominantly formed in a collinear reaction geometry, but for the latter reaction there is less restriction to a collinear geometry if the CH bond in HCN is highly vibrationally excited. The additional experimental measurements have changed our original picture of the reaction dynamics, namely with regard to the existence of complex formation[21] [gained from similar results of HCN(004) and HCN(302) reactions], now favoring a pure direct abstraction. The conclusion agrees with theoretical results of Harding[13] and Bair *et al.*[16] who predict the lowest energy route for both reactions to be a direct, collinear abstraction. The detailed information from our measurements offers a possibility for comparison with results obtained from quasiclassical trajectory studies or quantum mechanical calculations.

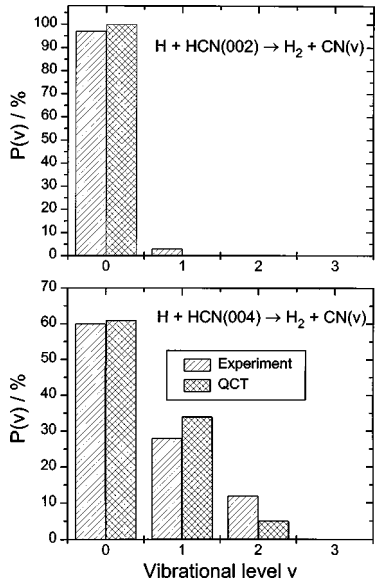

FIG. 13. Vibrational state distribution of CN for the reactions H+HCN(002) (upper part) and H+HCN(004) (lower part). Comparison of the results obtained from the experiment and the trajectory study is shown.

ACKNOWLEDGMENTS

We thank Professor F. J. Comes for helpful discussions and material support. C.K. thanks the Fonds der Chemischen Industrie for fellowship support. Financial support by the Deutsche Forschungsgemeinschaft is gratefully acknowledged.

[1] F. F. Crim, J. Phys. Chem. **100**, 12725 (1996).
[2] R. L. Vander Wal, J. L. Scott, and F. F. Crim, J. Chem. Phys. **94**, 1859 (1991).
[3] I. Bar, Y. Cohen, D. David, T. Arusi-Parpar, S. Rosenwaks, and J. J. Valentini, J. Chem. Phys. **95**, 3341 (1991).
[4] R. J. Barnes, A. F. Gross, and A. Sinha, J. Chem. Phys. **106**, 1284 (1997).
[5] J. D. Thoemke, J. M. Pfeiffer, R. B. Metz, and F. F. Crim, J. Phys. Chem. **99**, 13748 (1995).
[6] R. B. Metz, J. D. Thoemke, J. M. Pfeiffer, and F. F. Crim, J. Chem. Phys. **99**, 1744 (1993).
[7] M. J. Bronikowski, W. R. Simpson, and R. N. Zare, J. Phys. Chem. **97**, 2194 (1993).
[8] S. S. Brown, R. B. Metz, H. L. Berghout, and F. F. Crim, J. Chem. Phys. **105**, 6293 (1996).
[9] T. Arusi-Parpar, R. P. Schmid, R.-J. Li, I. Bar, and S. Rosenwaks, Chem. Phys. Lett. **268**, 163 (1997).
[10] J. Berkowitz, G. B. Ellison, and D. Gutman, J. Phys. Chem. **98**, 2744 (1994).
[11] M. J. Frost, I. W. Smith, and R. D. Spencer-Smith, J. Chem. Soc. Faraday Trans. **89**, 2355 (1993).
[12] I. R. Sims and I. W. M. Smith, J. Chem. Soc. Faraday Trans. II **85**, 915 (1989).
[13] L. B. Harding, J. Phys. Chem. **100**, 10123 (1996).
[14] J. de Juan, S. Callister, H. Reisler, G. A. Segal, and C. J. Wittig, J. Chem. Phys. **89**, 1977 (1988).
[15] H. Schacke, H. Gg. Wagner, and J. B. Wolfrum, Ber. Bunsenges. Phys. Chem. **81**, 670 (1977).
[16] R. A. Bair and T. H. Dunning, Jr., J. Chem. Phys. **82**, 2280 (1985).
[17] H. M. Lambert, T. Carrington, S. V. Filseth, and C. M. Sadowski, J. Phys. Chem. **97**, 128 (1993).
[18] G. W. Johnston and R. Bersohn, J. Chem. Phys. **90**, 7096 (1989).
[19] I. R. Sims and I. W. M. Smith, Chem. Phys. Lett. **149**, 565 (1988).
[20] Q. Sun and J. M. Bowman, J. Chem. Phys. **92**, 5201 (1990).
[21] C. Kreher, R. Theinl, and K.-H. Gericke, J. Chem. Phys. **104**, 4481 (1996).
[22] C. Kreher, R. Theinl, and K.-H. Gericke, J. Chem. Phys. **103**, 8901 (1995).
[23] J. M. Pfeiffer, R. B. Metz, J. D. Thoemke, E. Woods III, and F. F. Crim, J. Chem. Phys. **104**, 4490 (1996).
[24] R. B. Metz, J. D. Thoemke, J. M. Pfeiffer, and F. F. Crim, Chem. Phys. Lett. **221**, 347 (1994).
[25] Y. Matsumi, K. Tonokura, and M. Kawasaki, J. Chem. Phys. **97**, 1065 (1992).
[26] E. Jensen, J. S. Keller, G. C. G. Waschewsky, J. E. Stevens, and R. L. Graham, J. Chem. Phys. **98**, 2882 (1993).
[27] S. H. S. Wilson, M. N. R. Ashfold, and R. N. Dixon, J. Chem. Phys. **101**, 7538 (1994).
[28] H. Sasada, J. Chem. Phys. **88**, 767 (1988).
[29] K. R. German and W. S. Gornall, J. Opt. Soc. Am. **71**, 1452 (1981).
[30] A. M. Smith, S. L. Coy, and W. Klemperer, J. Mol. Spectrosc. **134**, 134 (1989).
[31] D. H. Rank and G. Skrinko, J. Opt. Soc. Am. **50**, 421 (1960).
[32] A. M. Smith and U. G. Jørgensen, J. Chem. Phys. **87**, 5649 (1987).
[33] A. E. Douglas and D. Sharma, J. Opt. Soc. Am. **21**, 448 (1953).
[34] D. Romanini and K. K. Lehmann, J. Chem. Phys. **102**, 633 (1995).

[35] D. Romanini and K. K. Lehmann, J. Chem. Phys. **99**, 6287 (1993).
[36] K. K. Lehmann, G. J. Scherer, and W. Klemperer, J. Chem. Phys. **77**, 2853 (1982).
[37] G. Herzberg, *Molecular Spectra and Molecular Structure II, Infrared and Raman Spectra of Polyatomic Molecules* (van Nostrand, New York), S. 215 f (1996).
[38] K. Mikulecky and K.-H. Gericke, J. Chem. Phys. **101**, 9635 (1994).
[39] P. R. Fleming and J. S. Hutchinson, J. Chem. Phys. **90**, 1735 (1989).
[40] A. Sinha, J. D. Thoemke, and F. F. Crim, J. Chem. Phys. **96**, 372 (1992).
[41] A. Sinha, M. C. Hsiao, and F. F. Crim, J. Chem. Phys. **94**, 4928 (1991).
[42] J. Wu, R. Huang, M. Gong, A. Saury, and E. Carrasquillo, J. Chem. Phys. **99**, 6474 (1993).
[43] P. R. Fleming and J. S. Hutchinson, J. Chem. Phys. **90**, 1735 (1989).
[44] D. C. Clary, J. Phys. Chem. **99**, 13664 (1995).
[45] H. M. Lambert, T. Carrington, S. V. Filseth, and C. M. Sadowski, J. Phys. Chem. **97**, 128 (1993).
[46] G. W. Johnston and R. Bersohn, J. Chem. Phys. **90**, 7096 (1989).
[47] R. N. Zare, Mol. Photochem. **4**, 1 (1972).
[48] R. N. Zare, Ber. Bunsenges. Phys. Chem. **86**, 422 (1982).
[49] E. Reinsch, K.-H. Gericke, and C. J. Kreher, J. Chem. Phys. **107**, 10567 (1997).
[50] H. J. Loesch, E. Stenzel, and B. Wüstenbecker, J. Chem. Phys. **95**, 3841 (1991).
[51] M. Hoffmeister, R. Schleysing, and H. J. Loesch, J. Phys. Chem. **91**, 5441 (1987).
[52] T. Takayanagi and G. C. Schatz, J. Chem. Phys. **106**, 3227 (1997).
[53] T. Takayanagi, Bull. Chem. Soc. Jpn. **68**, 2532 (1995).
[54] A. N. Brooks and D. C. Clary, J. Chem. Phys. **92**, 4178 (1990).
[55] Q. Sun and J. M. Bowman, J. Chem. Phys. **92**, 5201 (1990).
[56] D. C. Clary, J. Phys. Chem. **99**, 13664 (1995).
[57] S. Chapman, B. C. Garrett, and W. H. Miller, J. Chem. Phys. **64**, 502 (1976).
[58] G. C. Schatz and T. Mulloney, J. Phys. Chem. **83**, 989 (1979).
[59] G. C. Schatz, Top. Current Phys. **33**, 25 (1983).
[60] C. W. Eaker, G. C. Schatz, N. De Leon, and E. J. Heller, J. Chem. Phys. **81**, 5913 (1984).